

Microensing towards the LMC: self lensing for OGLE-II and OGLE-III

S. Calchi Novati^{1,2} \star and L. Mancini^{1,2,3}

¹ Dipartimento di Fisica “E. R. Caianiello”, Università di Salerno, Via Ponte don Melillo, 84084 Fisciano (SA), Italy

² Istituto Internazionale per gli Alti Studi Scientifici (IIASS), Vietri Sul Mare (SA), Italy

³ Dipartimento di Ingegneria, Università del Sannio, Benevento, Italy

date

ABSTRACT

We present an analysis of the results of the OGLE-III microlensing campaign towards the Large Magellanic Cloud (LMC). We evaluate for all the possible lens populations along the line of sight the expected microlensing quantities, number of events and duration. In particular we consider lensing by massive compact halo objects (MACHOs) in the dark matter haloes of both the Milky Way (MW) and the LMC, and “self lensing” by stars in the LMC bar and disc, in the MW disc and in the stellar haloes of both the LMC and the MW. As a result we find that the self-lensing signal is able to explain the 2 OGLE-III microlensing candidates. In particular, we estimate the expected MW disc signal to be almost as large as that from LMC stars and able, by itself, to explain the observed rate. We evaluate a 95% CL *upper* limit for f , the halo mass fraction in form of MACHOs, in the range 10-20% for $(10^{-2} - 0.5) M_{\odot}$, and $f = 24\%$ for $1 M_{\odot}$ (below 10% in this full range, and in particular below 5% for $(10^{-2} - 0.1) M_{\odot}$) for the Bright (All) samples of source stars. Furthermore, we find that these limits do not rise much even if we assume the observed events *are* MACHOs. For the All sample we also evaluate a rather significant constraint on f for larger values of the MACHO mass, in particular $f \sim 50\%$ (95% CL) for $100 M_{\odot}$, to date the stronger bound coming from microlensing analyses in this mass range. Finally, we discuss these results in the framework of the previous observational campaigns towards the LMC, that of the MACHO and the EROS collaborations, and we present a joint analysis of the OGLE-II and the OGLE-III campaigns.

Key words: Gravitational lensing: micro; Galaxy: halo; Galaxy: structure; dark matter

1 INTRODUCTION

Microlensing has been originally proposed by Paczyński (1986) as a tool to detect dark matter in form of (faint) massive compact halo objects (MACHOs) in the galactic haloes. Because of the small optical depth (we refer to Mao (2008) and references therein for an introduction to microlensing), dense stellar field has to be monitored to increase the rate of events. The more nearby available targets to look for MACHOs within the Galactic halo are the Magellanic Clouds (the LMC and the SMC), that have been therefore the objects of the first microlensing campaigns by the MACHO (Alcock et al. 1993), the EROS (Aubourg et al. 1993) and the OGLE (Udalski et al. 1993) collaborations and for which several results have been reported so far (for a recent review we refer to Moniez 2010). Meanwhile microlensing has moved on and currently is an established tool of investigation over a broad range of astrophysical issues, with one of the main focuses being currently the search and the characterization of extra solar planets (Bozza et al. 2011).

As for microlensing searches towards the Magellanic Clouds, previous analyses are in agreement to exclude MACHOs as a viable dark matter candidate for masses below $\approx (10^{-1} - 10^{-2}) M_{\odot}$. However, a relevant discrepancy still exists as for a possible population of compact halo objects in the mass range $(0.1 - 1) M_{\odot}$. The MACHO collaboration claimed for a halo mass fraction in form of MACHOs of about $f \sim 20\%$ out of observations of 13-17 microlensing candidate events towards the LMC (Alcock et al. 2000), a result more recently confirmed by Bennett (2005), who in particular confirmed the microlensing nature of 10-12 out of the original set of 13 candidate events. On the other hand, the EROS (Tisserand et al. 2007) and OGLE-II (Wyrzykowski et al. 2009, 2010), out of observations towards both the LMC and SMC, concluded by putting extremely severe *upper* limits on the MACHO contribution also in this mass range (in particular, the EROS collaboration reported an upper limit $f = 8\%$ for $0.4 M_{\odot}$ MACHOs). Finally, we recall that results on MACHOs through microlensing searches have been reported also from observational campaigns towards M31 (Calchi Novati 2010).

A source of debate for these results is the intrinsic *nature* of the reported microlensing events. Indeed, in order to draw mean-

\star E-mail: novati@sa.infn.it

ingful insights into the contribution of compact halo dark matter objects it is essential first to estimate accurately all the possible contributions due to (luminous) lenses belonging to known populations located along the line of sight. We refer to this possibility (first addressed by Sahu (1994) and thereby the objects of several investigations, among which Gyuk et al. 2000; Jetzer et al. 2002) as, broadly speaking, “self lensing”, to indicate any lens population that is not composed by MACHOs. A possibly non exhaustive list includes lenses belonging to the luminous components of the LMC which act also as sources (the disc and the bar), the disc of the MW and the somewhat more elusive stellar haloes for both the MW and the LMC.

Hints on the nature of single specific events require additional informations necessary to break the intrinsic degeneracies within the lensing parameter space. These may come from observed features along the microlensing light curves, as in binary systems, or by new independent measurements. This issue has been addressed for a few Magellanic Clouds events, and in particular for two SMC events both found to be attributed more likely to self lensing: the caustic crossing binary event MACHO 98-SMC-1 (analysed for instance by Alcock et al. 1999; Rhie et al. 1999), and MACHO 97-SMC-1, a long duration event for which a spectroscopic analysis of the source has been carried out by Sahu & Sahu (1998). On the other hand, the halo lensing solution is strongly favored for OGLE-2005-SMC-001 thanks to a space-based parallax measurement (Dong et al. 2007). The SMC is any case somewhat peculiar with respect to the LMC, both for its intrinsic density distribution and orientation, and a global analysis for the events detected along this line of sight is still missing. We also recall the LMC event MACHO-LMC-5, whose lens has been directly observed by means of the HST (Alcock et al 2001) and finally acknowledged to be a MW disk M-dwarf lying a distance at about 580 pc (Gould 2004; Gould et al. 2004; Drake et al. 2004), more likely to be attributed to the thick disc component also because of its proper motion.

A different approach to the same problem is that based on a statistical analysis of full set of events. Within this framework in previous analyses we have considered the set of events reported by the MACHO collaboration and shown that, on the basis of both their number and their characteristics (duration and spatial distribution), they can not all be attributed to self lensing (Mancini et al. 2004). In Calchi Novati et al. (2006) we have considered the possible role played by the LMC dark matter halo, and in particular we have challenged the current view that the halo fraction in form of MACHOs for the MW and the LMC are equal. In Calchi Novati et al. (2009) we have discussed the results of the OGLE-II campaign towards the LMC, confirming in particular the outcomes of Wyrzykowski et al. (2009) in that the observed rate was consistent with the expected self-lensing signal. Finally, Mancini (2009) has reconsidered microlensing towards the LMC by adopting a non-gaussian velocity distribution for the sources.

Here we report on a detailed analysis of the recent results of the OGLE-III campaign towards the LMC (Wyrzykowski et al. 2011). In particular we estimate the number of the expected events for all the possible lens population with the purpose to derive an accurate limit on the halo fraction in form of MACHOs. As a result, overall, we find the observed rate to be compatible with the expected self-lensing signal. The plan of the paper is as follows. In Section 2 we resume the main outcomes of the OGLE analysis, with in particular a discussion on the issue of blending (and a comparison with the MACHO and the EROS strategies). In Section 3 we present our analysis. After introducing, Section 3.1, our main tool of investigation, the microlensing rate, and the assumed astro-

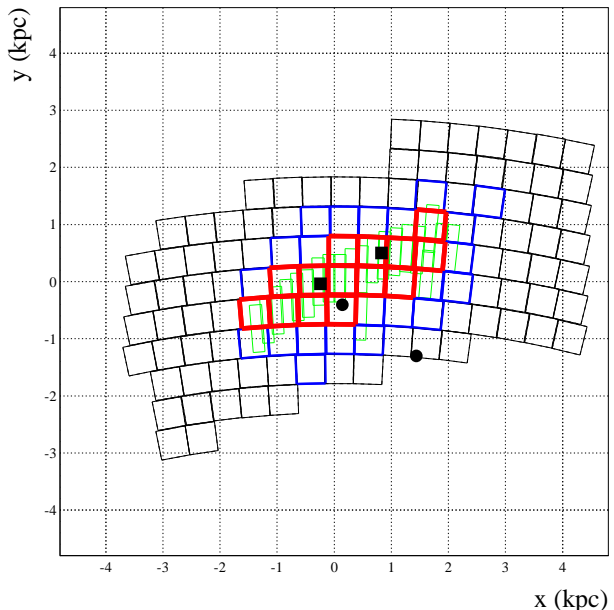


Figure 1. The field of view of the OGLE-II (thin lines in the innermost region) and OGLE-III campaigns towards the LMC. For OGLE-III the different contours are related to the number of monitored stars (see text for details), moving from the more crowded inner region to the more sparse stellar fields in the outer region of the LMC. The squares and the dots indicate the position of the reported microlensing candidates for the OGLE-II and OGLE-III campaigns, respectively (in particular, OGLE-LMC-03 is located at the boundary of the monitored region). The $x - y$ reference system has its origin at the centre of the LMC, the x -axis antiparallel to the right ascension and the y -axis parallel to the declination.

physical model, Section 3.2, in Section 3.3 we derive the expected microlensing quantities, number of events and duration. On the basis of this result, in Section 3.4 we discuss the possible nature of the reported observed events and in particular we evaluate the limits on dark matter in form of compact halo objects. Finally, in Section 4 we present our conclusions.

2 MICROLENSING OBSERVATIONS TOWARDS THE LMC: THE OGLE CAMPAIGNS

OGLE has continuously upgraded its set up moving on successively to OGLE-II, OGLE-III for finally recently entering in its OGLE-IV phase of evolution. In Fig. 1 we show the contours of the monitored fields of view towards the LMC for the OGLE-II and the OGLE-III campaigns (with overall 21 and 116 fields, respectively). Besides the observed fields, the relevant statistics that characterize an observational campaign are the overall duration, T_{obs} ; the number of monitored stars that act as potential sources for microlensing events, N_{obs}^* (sometimes the product of these two term is indicated as the overall “Exposure”, E). Finally, a selection pipeline is further specified by the maximum allowed value for the impact parameter, u_{MAX} and the *efficiency*, usually expressed as a function of the event duration, the *Einstein time*, $\mathcal{E} = \mathcal{E}(t_E)$.

In Table 1 we report the main statistics for the OGLE-II and OGLE-III experimental set up and selection pipeline (in both cases, $u_{\text{MAX}} = 1$). We further discuss the underlying rationale for the two sets of sources, All and Bright samples, below. In particular, the improvement of the available statistics given by OGLE-III with

Table 1. Characteristics of the OGLE-II and OGLE-III observational campaigns towards the LMC: overall duration of the experiment, number of monitored (estimated) sources, both Bright and All samples (see text for details), and overall field of view.

	duration	N_{obs}^*		fov
	(days)	All	Bright	(deg ²)
		$\times 10^6$		
OGLE-II	1428	11.8	3.6	4.5
OGLE-III	2850	22.7	6.3	40

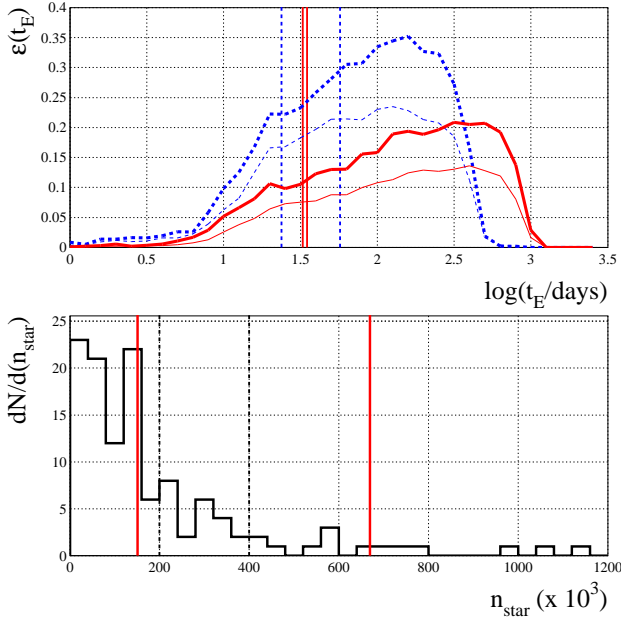


Figure 2. Top: Detection efficiency as a function of the Einstein time for OGLE-III, field 163 (solid lines) and OGLE-II, field 4, for the Bright (bold) and All star samples (OGLE-III field 163 partly overlaps OGLE-II field 4). The solid (dashed) lines indicate the reported duration for the candidate events for the OGLE-III (OGLE-II) campaigns. Bottom: Distribution for the number of star per field for the 116 OGLE-III LMC fields. The solid lines indicates the location of the fields for which the detection efficiency has been evaluated (corresponding to the fields where the microlensing candidate events have been observed). The dotted lines delimit the three bins we have used in the analysis (see text for details).

respect to OGLE-II both in term of the experiment duration and number of potential sources, is apparent. In Fig. 2 (top) we show $\mathcal{E}(t_E)$ for the inner OGLE-III field 163, and the partly overlapping OGLE-II field 4. As apparent, there is a significant decrease in the OGLE-III efficiency, in particular in the range of t_E values corresponding to those of the observed candidate events (Table 2). This explains, as detailed in the next Sections, the reason of the relatively small increase in the expected number of events for the OGLE-III campaign compared to OGLE-II.

Wyrzykowski et al. (2011) for their OGLE-III analysis have reported the evaluation of the efficiency for only the two fields of view (rather, for one CCD out of eight per each of these two fields) where the events have been observed: field 163 and 122 located respectively in the central and in the outer LMC region. In particular, moving towards the outer LMC regions the fields gradually become less dense, with fewer observed objects. A reliable measure of the

crowdness of the fields is given by the number of estimated sources per field. In Fig. 2 (bottom) we show the histogram of these values as reported by Wyrzykowski et al. (2011). Wyrzykowski et al. (2011) remarked that the efficiency is larger in less crowded fields, and this turns out to be by about a factor between 2 and 3 for field 122 with respect to field 163 (both for the All and the Bright samples of stars, at least for $t_E > 10$ days, see discussion below). Accordingly, for our analysis, we evaluate the efficiency in each field, given the number of sources, making use of a linear interpolation¹. for each value of t_E . In the innermost and outer LMC regions, to avoid extrapolation, we use the value of the efficiency for fields 163 and 122, respectively (extrapolation would in fact quickly lead to unreasonable small values for the efficiency in the inner LMC region, whereas in the outer region whatever choice is almost irrelevant as the expected rate, following the decrease in the number of sources, quickly drops to very small values).

For small values of the duration t_E , below about 5-10 days, the efficiency drops quickly below 10% down to 0. This makes OGLE-III, as well as OGLE-II, rather insensitive to MACHOs with masses below about $10^{-3} M_{\odot}$, for which in particular the expected durations, not corrected for the efficiency, are below 2 days. Furthermore, the statistics of the simulated light curves used to evaluate $\mathcal{E}(t_E)$ is increasingly poor moving towards smaller values of t_E so that all the results there should be taken with some care. In particular, contrary to the average result also reported above, the efficiency turns out to be larger in the inner, more crowded, field 163 with respect to the outer field 122 for $t_E < 5$ days.

The overall large field of view monitored by OGLE-III towards the LMC, going from the inner more crowded region to the outer sparse field, can be exploited to carry out analyses based on the spatial distribution. In the following we are going to make use of this chance, in particular we identify three bins based on the number of estimated sources per field: the inner 14 fields with $N_{\text{obs}}^* > 400 \times 10^3$ (corresponding roughly to the region monitored by OGLE-II), the 22 “intermediate” fields with $200 < N_{\text{obs}}^* < 400 \times 10^3$ and the outer 80 fields with $N_{\text{obs}}^* < 200 \times 10^3$ (to which we refer to also as bin 1, 2 and 3, respectively, Figs. 1,2).

In Table 2 we report the informations on the microlensing candidate events for the OGLE-II (Wyrzykowski et al. 2009) and OGLE-III (Wyrzykowski et al. 2011) campaigns towards the LMC. Comparing to our mentioned choice for the bin in the spatial distribution, we see that one event is located within the inner bin (OGLE-LMC-04), while the second event (OGLE-LMC-03) is located within the outer bin at the very boundary of the overall monitored fields (Fig. 1).

The choice for the two sets of source stars (and the two parallel corresponding microlensing search pipelines), to which OGLE refers to as the All and the Bright samples, is related to the issue of blending. The term *blending* indicates that usually more than one star is enclosed within the seeing disc of a given resolved object whose light curve is searched for microlensing variations (this is opposed to the *pixel lensing* regime (Gould 1996) where one looks for flux variations of *unresolved* sources, as for instance towards M31). Blending complicates the analysis because, first, the real number of sources is therefore larger than the number of ob-

¹ The reliability of this approximation scheme is supported by the fact that the OGLE-III observational sampling, besides the field crowdness a driving element of the observational setup for the determination of the efficiency, was relatively uniform over all the LMC fields (Ł. Wyrzykowski, private communication)

Table 2. Microlensing candidate events for the OGLE-II and OGLE-III observational campaigns towards the LMC.

event	RA [J2000.0]	Dec [J2000.0]	t_E [days]	field #
OGLE-LMC-01	5:16:53.26	-69:16:30.1	57.2	8
OGLE-LMC-02	5:30:48.00	-69:54:33.6	24.2	2
OGLE-LMC-03	5:07:03.63	-71:17:06.3	35.0	122
OGLE-LMC-04	5:25:39.58	-70:19:49.7	32.8	163

served objects; second, it can make unreliable the estimate of the microlensing parameters, in particular the duration t_E . These effects somewhat tend to compensate one each other for the evaluation of the optical depth, nonetheless blending remains a main issue of concern for the interpretation of microlensing results. Indeed, only the acknowledgement and then a deeper understanding of this problem lead finally to reconcile theory and observations for the optical depth evaluations towards the Galactic bulge, (Popowski et al. 2005; Sumi et al. 2006; Hamadache et al. 2006) for the final analyses of the MACHO, OGLE and EROS collaborations, respectively (we also recall the previous analysis of the MOA group (Sumi et al. 2003) who used a Monte Carlo simulation to address the issue of blending and we refer to Calchi Novati et al. (2008) for a discussion on the microlensing *rate* for Galactic bulge observations). The strategy adopted to minimize blending was to take as potential sources only a subset of the *brighter* observed objects. In particular, for these Galactic bulge searches, the sources were selected in a well defined region of the color-magnitude-diagram (CMD) in order to select, as best as possible, only *Bulge* (red) clump giants. In fact, Sumi et al. (2006), as opposed to the MACHO and EROS analyses, already stressed the extent to which blending was relevant also for these bright objects, an issue further analysed in Smith et al. (2007), to which we refer for a more through discussion. Following the underlying rationale of these Galactic bulge analyses, a similar strategy was then adopted also by EROS for his final LMC analysis (Tisserand et al 2007), with however a somewhat looser cut within the CMD specified only with the request for the source objects to be brighter than a given threshold, with a value varying with the field. In the inner region the threshold magnitude was fixed at $R_{\text{EROS}} \sim I_{\text{OGLE}} = 18.2$, whereas fainter threshold values, by more than about 1 mag, were allowed for in the outer LMC region. This allowed to include as viable sources, besides the clump giant region, also, in particular, both redder giants and very bright main sequence stars. This way EROS reduced the number of sources down to about 20% of the original set, with $N_{\text{obs}}^* = 5.5 \times 10^6$ spread over its (huge) LMC field of view of about 84 deg^2 . On the other hand the MACHO collaboration for his final analysis of 5.7 years of data (Alcock et al. 2000) had chosen a different strategy allowing also for faint sources. Furthermore, MACHO looked mostly at the inner, and denser, LMC region with for an overall field of view of 13.4 deg^2 . The MACHO detection efficiency (Alcock et al. 2001) was then specifically designed to hold for a total exposure of $E \equiv N_{\text{obs}}^* \cdot T_{\text{obs}} = 6.12 \times 10^7 \text{ object-years}$ (rather than for stars), for 11.9×10^6 observed objects, with an estimated mean value stars (brighter than $V = 24$) per object of 10.84 ± 2.4 . In particular, the reported efficiency was found to vanish for unresolved stars fainter than $V \sim 24$ (while observing objects down to $V \sim 22$). We recall that the difference in their respective strategies, looking down to faint viable sources in the inner LMC region (MACHO), rather than for bright sources only

Table 3. Mean and rms values of the ratio of the estimated number of (estimated) real stars over the number of observed objects, for the three bins we have identified to trace the spatial distribution of the OGLE-III LMC monitored region (bin 1, 2 and 3 moving from the inner to the outer LMC region, see text for details). We also note that the ratio of the estimated number stars, Bright over All sample, is roughly constant across the fields, though rising towards the outer region (0.26 ± 0.03 , 0.28 ± 0.02 and 0.30 ± 0.03 for bins 1, 2 and 3, respectively).

Bin number	All sample	Bright sample
bin 1	1.27 ± 0.08	1.14 ± 0.04
bin 2	1.13 ± 0.03	1.07 ± 0.02
bin 3	1.06 ± 0.02	1.02 ± 0.01

across a much more extended field of view (EROS), has already been considered as a possible way out to explain the discrepancy already mentioned above in their results as for the compact halo objects fraction in the mass range $(0.1 - 1) M_{\odot}$ (Moniez (2010) and references therein). For this reason the mentioned choice of OGLE, which we now discuss in more detail, looks promising to better address this issue.

The strategy adopted by OGLE for its final LMC analyses, similar for both OGLE-II and OGLE-III, has been to carry out two parallel microlensing search pipelines on two distinct sets of sources. The All sample, for objects down to a limit threshold magnitude of $I_C = 20.4$; and a Bright sample composed by a $\sim 30\%$ subset of the brighter sources with threshold magnitude fixed at 1 mag fainter than the CMD red clump center ($I_C = 18.8$ for their reference field LMC_SC1, located in the innermost LMC region). Through an analysis of the underlying luminosity function, OGLE estimated the number of source *stars* per observed *object* down to a magnitude $I = 23.9$ (23.4) for OGLE-II (OGLE-III) respectively. As a measure for the impact of blending, we report (Table 3) the ratio of the number of stars per object for the three bins in the spatial distribution already introduced. As to be expected, blending is more relevant in the crowded inner LMC region (bin 1), with 1.27 (1.14) stars per object for the All (Bright) sample, respectively (we recall that for OGLE-II the corresponding reported values were 2.1 and 2.9^2). In particular, we find worth pointing out the extent to which blending is reported to be significant also for the Bright sample, in fact almost at the same level of the All sample (with a relative difference of only about 10%, both for OGLE-II and OGLE-III). A possible reason behind this outcome is the strategy of OGLE, its choice for the threshold magnitude values for the All and Bright samples, which appears somewhat intermediate comparing to the MACHO and EROS strategies. In particular, the OGLE threshold magnitude for the All sample is brighter than that of MACHO (to compare with V band values of the MACHO analysis we recall that the color for the red clump center, where most source are located, is $V - I \sim 1.0$), while the OGLE threshold magnitude for the Bright sample is fainter than that of EROS. Next observational campaigns, in particular the ongoing OGLE-IV, might hopefully further address this issue.

² The reason behind the smaller values reported for OGLE-III should be looked into a combination of effects: first and more important the better image quality of OGLE-III; then the 0.5 magnitude difference for the threshold value, and finally the refined OGLE-III analysis used to determine the underlying luminosity function (Ł. Wyrzykowski, private communication).

3 ANALYSIS

3.1 The microlensing rate

Microlensing observations offer two main tools of investigation to compare observations with the expected signal and accordingly draw conclusions on the astrophysical issues of interest: the optical depth, τ , and the microlensing rate, Γ (Mao 2008). The first is the instantaneous probability to observe a microlensing event, and therefore a *static* quantity. In particular, τ is directly related to the overall lens population density distribution but it turns out to be independent from the lens *mass*, one of the more crucial parameters one is usually interested to. This is at the same time a bonus, as it makes τ less model-dependent, and a limit, as it does not allow one to actually characterize the observed events. To this purpose the microlensing rate is therefore the quantity of choice being a *dynamic* quantity which allows one to compute the number of microlensing events per unit time for a given number of monitored stars. In particular, through the analysis of Γ , one can estimate the *number* of the expected events, N_{exp} , and their characteristics, more notably their *duration* and *spatial position*:

$$N_{\text{exp}} = N_{\text{obs}}^* T_{\text{obs}} \int dt_E \frac{d\Gamma}{dt_E} \mathcal{E}(t_E), \quad (1)$$

where we have explicitly taken into account of the experiment detection efficiency and written the rate in differential form (which provides also the expected duration distribution for the events).

Microlensing observations, at least for the more usual lensing configuration of single point source and point lens with uniform relative motion, allow one the estimate of a single physically relevant quantity, the event duration t_E , which is a function of the lens and source distances, the lens mass and the modulus of the lens-source relative transverse velocity which relates the Einstein radius, the microlensing event cross section, to the Einstein time, $v_t = R_E/t_E$. As distances, velocities and lens mass are not directly observable, one has to assume a model for all these quantities to integrate them out. The details of the models we use, as well as details on the evaluation of the microlensing rate, are discussed in our previous works, and in particular we refer to Calchi Novati et al. (2009) for a discussion on all the possible source and lens population we consider: for the sources, disc and bar LMC stars; for the lenses, disc and bar LMC stars (a case to which we refer in particular as “LMC self lensing”), Galactic disc stars and finally stars of both the LMC and the Galaxy stellar haloes, all of these lens populations contributing to “self lensing”; finally, for MACHO lensing, compact halo objects for both the MW and the LMC dark matter haloes.

3.2 The astrophysical model

The modelling of the LMC, in particular of its luminous components, is an extremely live subject of research. Our model, as described in detail in Mancini et al. (2004), is mainly based on the work of van Der Marel and collaborators (van der Marel et al. (2002) and references therein), whose conclusions have been challenged by several authors (see for instance the recent analyses of Subramanian & Subramaniam (2010); Bekki (2011) and references therein). It is beyond the purpose of the present analysis to further address this issue. This is because, as we detail in the following, our main results with respect to compact halo objects, are almost insensitive to the exact amount of the LMC self-lensing contribution. The same argument applies also with respect to the stellar haloes, with the additional caveat that their modeling is even more

problematic. In particular, for the LMC stellar halo (that giving the larger contribution of the two), here we use our Calchi Novati et al. (2009) “fiducial” model based on the analysis of Alves (2004). As also discussed in Calchi Novati et al. (2009), the more recent analysis of Pejcha & Stanek (2009) suggests a different spatial distribution for this component that may indeed significantly enhance the microlensing signal.

A fully detailed knowledge of the stellar structure of the MW is still lacking. To our purposes, the relevant quantities are the local stellar density and the vertical distribution. An accurate modelling becomes particularly important for a survey as OGLE-III where MW disc lensing can be expected, besides LMC self lensing, to give a relevant contribution to the rate. As we further address in the following sections, this is because of the broader spatial distribution of the expected MW disc signal, beyond the inner LMC region, with respect to that expected from LMC lenses. For this reason we update the model used in Calchi Novati et al. (2009). We assume a standard double exponential disc model (Dehnen & Binney 1998) with scale length R_d and scale height h_z , summing a thin disc and a thick disc component. Following the detailed stellar mass budget of Kroupa (2007) we fix the thin disc *stellar* central density to $\rho_{\text{thin},\odot} = 0.044 \text{ M}_{\odot} \text{pc}^{-3}$, to be compared for instance with $0.038 \text{ M}_{\odot} \text{pc}^{-3}$ in Flynn et al. (2006). For a scale height $h_{z,\text{thin}} = 250 \text{ pc}$ this gives a local disc column density $\Sigma_{\text{thin}} = 22 \text{ M}_{\odot} \text{pc}^{-2}$ (we do not consider the luminous *gas* component that does not lens). To complete our fiducial thin disc model we fix $R_{d,\text{thin}} = 2.75 \text{ kpc}$. Larger values of h_z are also reported. For instance, $h_{z,\text{thin}} = 300 \text{ pc}$ (Juric et al. 2008) would lead to $\Sigma_{\text{thin}} = 26.4 \text{ M}_{\odot} \text{pc}^{-2}$. The details of the model for the thick disc are less well constrained. This is important for microlensing as the larger scale height of this component is expected to significantly enhance the signal (Gould 1994; Gould et al. 1994). Here we follow the recent analysis of de Jong et al. (2010) and we take as our fiducial model $\rho_{\text{thick},\odot} = 0.0050 \text{ M}_{\odot} \text{pc}^{-3}$, $h_{z,\text{thick}} = 750 \text{ pc}$, summing up to $\Sigma_{\text{thick}} = 7.5 \text{ M}_{\odot} \text{pc}^{-2}$, and $R_{d,\text{thick}} = 4.1 \text{ kpc}$. These values, also compatible with the analysis of Juric et al. (2008), indicate a quite substantial thick disc over thin disc local density fraction, f_{thick} , here $f_{\text{thick}} = 11\%$ (together with a relatively small scale height) compared to previous analyses where values in the range $f_{\text{thick}} = 1\% - 10\%$ were reported (we refer to the discussion in Juric et al. (2008); de Jong et al. (2010) and references therein). As an extreme case of a “light” thick disc we will report also the results for $f_{\text{thick}} = 1\%$. For the thin (thick) disc component we assume a line-of-sight velocity dispersion of 30 km/s (40 km/s), respectively.

3.3 Expected events number and duration

The starting point of our analysis is the evaluation of the differential microlensing rate, which enters in Eq. 1, towards (the center of) all the 116 OGLE-III fields. This allows us to characterize the expected microlensing signal, in particular the events duration and number, that we now discuss in turn.

Useful insights can in fact be gained already by an analysis of the optical depth. We have addressed this issue in our previous papers (Mancini et al. 2004; Calchi Novati et al. 2009). Here we recall that a main difference for the optical depth maps for MW and LMC lens populations is that the contour levels of those for MW lenses are almost constant across the LMC field of view. This is explained by the geometry of the configuration, with the lenses being so close to the observer (a few kpc or even less, so that the spatial lens density distribution remains approximately constant across

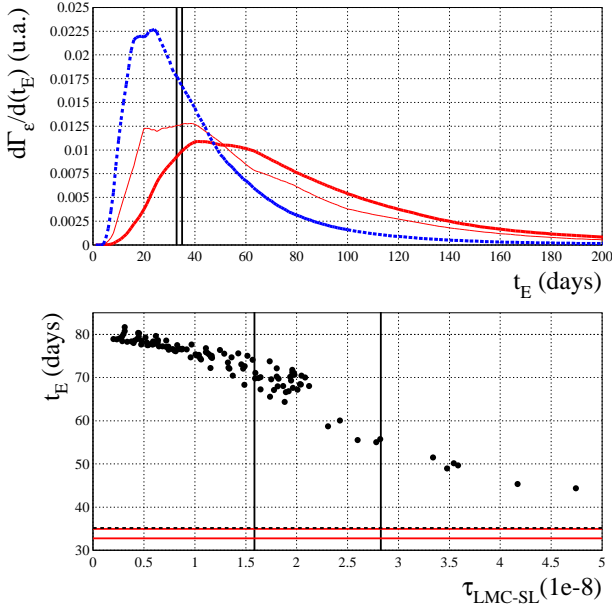


Figure 3. Top: The differential rate, $d\Gamma/dt_E$, corrected for the efficiency and normalized, for LMC self lensing evaluated along the line of sight towards the OGLE-III observed events (solid bold and thin line for OGLE-LMC-03 and OGLE-LMC-04, respectively), and for MW disc lenses (dashed line). The vertical solid lines indicate the values of the duration for the two OGLE-III observed events. Bottom: The expected median duration (corrected for the efficiency) for LMC self-lensing events for the 116 OGLE-III fields as a function of the corresponding value of the LMC self-lensing optical depth. The vertical lines correspond to the optical depth values towards the observed events, the solid horizontal lines indicate the values of the duration for the two OGLE-III observed events. The dotted horizontal lines indicates the expected values for MW disc lenses.

the full monitored field of view), and the lens distance being so small compared to the source distance. Coming to the microlensing rate, this outcome translates in particular into the very small variations for the expected event duration across the LMC field of view (Calchi Novati et al. 2009). (This does not apply, however, when moving to the expected number of events where the source density spatial distribution, strongly peaked at the LMC center, comes into play.) On the other hand, the differential rate, and the expected duration, vary quite significantly for the LMC lens populations, and this holds in particular for the LMC self lensing, with shorter duration expected in the inner LMC region. This is made apparent in Fig. 3, top panel, where we report the, efficiency-corrected and normalized, differential LMC self-lensing rate calculated along the direction towards the two observed events (located one in the inner and one in the outer LMC region), together with the MW disc rate. The plot makes also clear the rather large variance of these distributions. A more global picture is given in Fig. 3, bottom panel, where we report, always for LMC self lensing, the expected median duration as a function of the optical depth (providing a stronger correlation than the distance from the LMC center). As a median value for the expected duration (corrected for the OGLE efficiency) we find, for LMC self lensing, values in the range 45-80 days, with shorter duration expected in the central region; for MW disc lenses (both thin and thick components), about 40 days; for compact halo objects the duration varies with the assumed mass. For 0.1, 0.5 and $1.0 M_\odot$ MW MACHOs we evaluate an expected median duration of 21, 41 and 56 days, respectively. Furthermore, as already pointed

Table 4. Expected number of events for the luminous lens populations we consider (SL and SH stand for self lensing and stellar halo, respectively). N_{exp} is reported as the sum over the contribution of all the 116 OGLE-III fields (first two column) and the 21 OGLE-II fields (these results are reported from our previous analysis in Calchi Novati et al. 2009) for both the Bright and the All samples of sources.

lenses	OGLE-III		OGLE-II	
	BRIGHT	ALL	BRIGHT	ALL
LMC SL	0.63	1.60	0.46	1.10
MW disc	0.45	1.14	0.06	0.12
LMC SH	0.20	0.51	0.09	0.20
MW SH	0.09	0.24	0.03	0.07
total	1.37	3.49	0.64	1.49

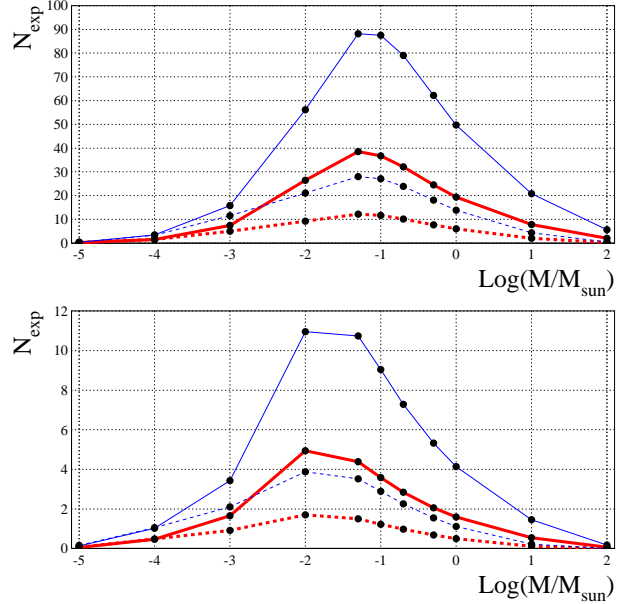


Figure 4. Expected number of MACHO lensing events for OGLE-III (OGLE-II) campaigns (solid and dashed lines, respectively), for both the MW (top) and the LMC dark matter haloes, the for the Bright (bold) and the All samples of stars.

out in Calchi Novati et al. (2006), LMC dark matter halo lenses are expected to give, for a given MACHO mass, shorter duration than Galactic MACHOs, with in particular $0.2 M_\odot$ LMC MACHOs expected to have similar duration than $0.5 M_\odot$ MW MACHOs.

Moving with our analysis to the expected number of events, in Table 4 we report the number of expected events for the luminous populations considered, for both the All and the Bright samples of stars. Taking into account the detection efficiency, in Fig. 4 we show the expected number of events for MACHO lensing, both MW and LMC, for a set of delta mass function.

In Table 4 and Fig. 4 we also report the expected number of events of the OGLE-II LMC campaign as evaluated in our previous analysis (Calchi Novati et al. 2009) (for MW disc lenses, using the same model as in Calchi Novati et al. (2009) we would have found, for OGLE-III, an expected signal of 0.17 and 0.43 events, for the Bright and the All sample, respectively). At first glance, a somewhat striking result is a relatively overall small increase of the expected number of events moving from OGLE-II to OGLE-III, when

taking into account the overall longer duration and larger number of sources, almost a factor of two each (Table 1), both entering linearly into the expression for evaluating the expected number of events (Eq. 1). As discussed in Section 2, the first and essential reason behind this result should be looked into the smaller detection efficiency reported for OGLE-III.

The expected number of MW disc lensing is 0.45 and 1.14, for the Bright and All sample respectively (about 70% of the expected LMC self lensing signal), to which the thick disc component contributes to about 50%. With reference to the discussion on the model in Section 3.2, we note that this fraction would drop below 10% for $f_{\text{thick}} = 1\%$, (and overall the MW disc over LMC self lensing signal to 40%). On the other hand, for a thin disc scale height of 300 pc we would get to an expected number of events, for the Bright and All sample respectively, of 0.54 and 1.38, almost 90% of the LMC self lensing signal. In any case, among the contributions to self lensing, these values make apparent the relevance of the MW disc signal with respect to the LMC self lensing signal.

Systematic uncertainties related to the assumed astrophysical model, besides those detailed for that of the MW disc, are to be expected in particular for the other prominent luminous lensing population, the LMC stars. We have addressed this issue in a previous analysis (Mancini et al. 2004). For somewhat extreme models of LMC, both structure and kinematic, we found variations in the expected number of events up to 30%-50%.

The expected number of events is related, besides to the lens population under exam, to the underlying source density distribution. Together, these elements determine the expected spatial distribution of the microlensing events. For a large enough set of events the spatial distribution becomes an extremely powerful tool of analysis to better address an essential problem of this analysis, namely the understanding on the nature of the observed events (as we did in our previous analyses of the MACHO events in Mancini et al. 2004; Calchi Novati et al. 2006). For the present analysis of the OGLE-III results, with only 2 observed events, we can not expect this analysis to give unambiguous outcomes. We may however take advantage of the rather large overall field of view of the OGLE-III fields across the LMC to at least address this issue and gain some insight into the problem. As introduced in Section 2, based on the number of the sources, which traces the underlying LMC populations, we address this issue by identifying 3 bins within the monitored OGLE-III region. Moving towards the outer LMC region, each bin is composed by 14, 22 and 80 OGLE-III fields, with a total fraction of sources per bin of 42%, 27% and 31%, respectively. The rationale behind this choice is that the innermost bin roughly corresponds to the innermost LMC region (where in particular the OGLE-II fields were distributed) whereas the two outer bins are chosen so to have, overall, roughly the same number of sources. The strong variation into the number of sources per field, moving from the crowded inner region to the more sparse LMC outskirts, is clearly reflected in the increasing number of fields per bin. The expected spatial distribution according to this bin choice is given in Table 5 where we report the fractions of the expected number of events per bin per each lens population considered. The outcome is driven by two competitive effects: the larger number of sources towards the LMC centre against the corresponding decrease for the detection efficiency. The other aspect is related to the lens spatial distribution, with LMC lenses more concentrated in the innermost region and MW lenses almost uniformly distributed across the monitored field of view. As a result, the LMC self-lensing signal is, as expected, more concentrated in the inner bin, where we find about 50% of the expected signal. For the other lens populations, in

Table 5. Microlensing rate analysis: fraction of the expected number of events for all the lens populations we consider (SL and SH stand for self lensing and stellar halo, respectively) for the 3 bins across the OGLE-III fields chosen to trace the spatial distribution (bin 1, 2 and 3 moving from the inner to the outer LMC region, see text for details).

lenses	fraction of N_{exp}		
	bin 1	bin 2	bin 3
LMC SL	0.484	0.273	0.244
MW disc	0.262	0.311	0.426
LMC SH	0.340	0.363	0.297
MW SH	0.261	0.314	0.425
MW halo	0.260	0.315	0.426
LMC halo	0.282	0.340	0.378

particular for MW disc lenses, we find a more smooth distribution, with roughly 30%, 30% and 40% of the expected events moving from the inner to the outer bin (the mean number of events per field, however, is as expected strongly peaked in the central LMC region).

This bin-based analysis offers also a second key of understanding on the relatively small increase of the number of events in OGLE-III with respect to OGLE-II. In particular we find the MW disc signal to increase for a much larger factor (about 3) with respect to LMC self lensing (with a relative increase of only a factor about 1.5). The reason behind lies into the already discussed much stronger concentration of LMC self lensing in our innermost LMC bin (corresponding also roughly to the OGLE-II fields) with respect to the more smoothly distributed MW disc signal.

3.4 The nature of the observed events

On the basis of the analyses carried out in the previous Section we can attemptively draw some conclusions on the nature of the observed signal. Both OGLE-III events, with a duration of about 30 days, fall at the inferior limit of the expected duration distribution for LMC self-lensing events (Fig. 3). This holds in particular (because of the correlation of the expected duration with the distance from the LMC center, Fig. 3 top panel), for the outer event OGLE-LMC-03, for which we find only 13% of the expected events with expected shorter duration. This fraction rises to 19% for the inner event, OGLE-LMC-04. The observed durations nicely match, on the other hand, the expected values for Galactic disc events (median value about 40 days). The observed event durations are also in agreement with expected Galactic MACHOs, in the mass range $(0.1 - 1) M_{\odot}$ (median value from 21 up to 56 days). Furthermore, as already remarked, for the Galactic lens populations, the expected duration has a rather uniform distribution across the entire LMC field of view, which is also in agreement with the observed values.

The analysis on the number of expected events on the other hand, Table 4, indicates that LMC self lensing alone can explain the 2 reported microlensing candidates. This holds for the All sample ($N_{\text{exp}} = 1.60$), but also, even if this case is somewhat more contrived, for the Bright sample (for $N_{\text{exp}} = 0.63$ we evaluate, according to a Poisson distribution, a 13% probability to find more than 2 events). These conclusions are supported by the analysis of the spatial distribution. In fact, the strong decrease of the LMC self-lensing rate in the outer LMC region is at least partially compensated by the extremely large number of observed fields. In particular, even if almost half of the events are expected in the central

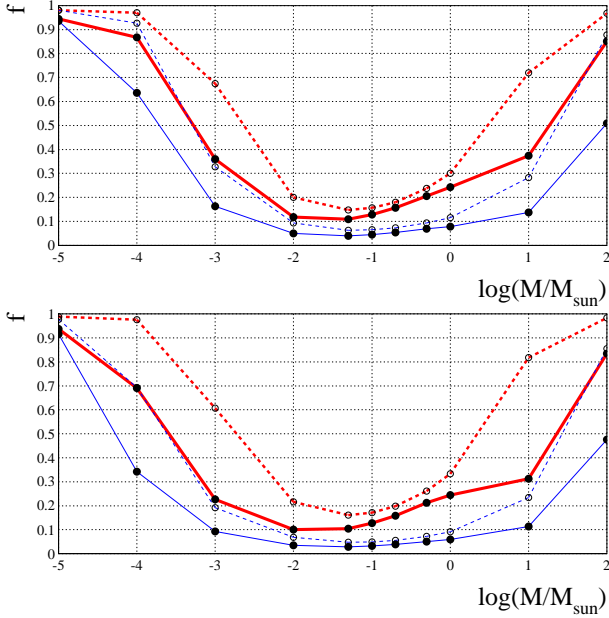


Figure 5. The 95% CL upper limit for the halo mass fraction in form of MACHOs as a function of the MACHO mass. Bold and thin lines for the Bright and the All samples of stars, respectively. Dashed lines indicate the limit when we assume the observed events *are* MACHOs. Top: results of the OGLE-II campaign, bottom: results for the joint analysis of the OGLE-II and OGLE-III campaigns. The analysis is based upon the likelihood function given in Eq. 2, where in particular we take into account both the MACHO lensing and the self-lensing populations.

14 LMC fields, corresponding to the inner bin in our division (Table 5), still 0.40 (0.15) events are expected in the outer bin, giving a probability of 32% (14%), for the All (Bright) sample, respectively, to observe more than 1 event into the outer bin.

The analysis on the expected number of events from MW disc lenses, on the other hand, supports the hint coming from the analysis on the duration. In fact, with $N_{\text{exp}} = 1.14$ and 0.45 for the All and bright sample, respectively, MW disc lenses by themselves could explain both reported events almost at the same level of confidence than LMC star lenses. This explanation would be, however, even more contrived for the Bright sample (with a 8% probability to observe more than 2 events, a value that would drop below 3% assuming the “light” thick disc model). As for the spatial distribution, the situation is inverse with respect to the LMC self lensing case, with now the reported candidate in the inner bin more difficult to be explained. Still, we evaluate a probability of 26% (12%), for the All (Bright) sample, respectively, to observe more than 1 MW disc event into the inner bin.

All the above considerations can be made more quantitative taking furthermore into account simultaneously all the possible lens populations and the characteristics of the reported candidate events through a likelihood analysis. In particular, by Bayesian inversion, this allow us to evaluate, for a given MACHO mass, the probability distribution for the halo mass fraction in form of MACHO, $P(f)$ (we consider a constant prior for f different from zero in the interval $(0,1)^3$).

$$L(f, m) = \exp(-N_{\text{exp}}(f, m)) \prod_{i=1}^{N_{\text{obs}}} \left. \frac{d\Gamma_{i,\mathcal{E}}}{dt_E} \right|_{t_{E,\text{event}}}, \quad (2)$$

where $\Gamma_{\mathcal{E}}$ is the microlensing rate corrected by the detection efficiency, $d\Gamma_{\mathcal{E}}/dt_E = d\Gamma(t_E)/dt_E \cdot \mathcal{E}(t_E)$. The expression reported in Eq. 2 for the likelihood allows one to take explicitly into account the observed duration as well as the event position as the differential rate is evaluated along the direction towards the events. Here both N_{exp} and the differential rate $d\Gamma_{\mathcal{E}}/dt_E$ are to be intended as given by the sum over all the possible lens populations, with the MACHO lensing contributions multiplied by the factor f . In principle it is possible to rewrite Eq. 2 by taking directly into account bins in distance from the LMC center (similarly for instance to the pixel lensing M31 analysis discussed in Calchi Novati et al. (2005)). Following the bin choice of the previous Section we have found this analysis not to lead to any substantial change in the results.

The results of the likelihood analysis are reported in Fig. 5 where, for given MACHO mass, we show the limits for the halo mass fraction on form of MACHOs, f . In particular, for the Bright star sample we evaluate a 95% CL *upper* limit well below 20% in the mass range $(10^{-2} - 2 \times 10^{-1}) M_{\odot}$, and below 10% up to $1 M_{\odot}$ for the All star sample.

Self lensing, as discussed, can account for both observed events, however, to the purpose of the evaluation of the limits on f , it must be acknowledged that it does not have a leading role. In fact, it is the number of expected MACHO lensing (Fig. 4), at least in the MACHO mass range $(10^{-2} - 1) M_{\odot}$, as compared to the number of reported microlensing candidate, that leads to firmly exclude a significant contribution of this population. This is apparent by inspection of Fig. 5 (dashed lines) where we show the results of the likelihood analysis assuming both the observed events *are* MACHOs: the increase with respect to the case where we include also self lensing is of a few percent only. In that case it makes sense, in principle, to evaluate also a *lower* limit for f , which we find to vary in the range $f \sim (2 - 4)\%$ in the MACHO mass range $(10^{-2} - 1) M_{\odot}$ (for the Bright star sample).

Finally, we perform a joint likelihood analysis for the OGLE-II and OGLE-III campaigns (Fig. 5, bottom panel). As a result we find the upper limits on f , almost unchanged (with in particular a marginal decrease for the All sample of stars). Comparing to the results discussed in Calchi Novati et al. (2009) this reflects the larger statistics achieved during the OGLE-III campaign compared to the OGLE-II one.

Our results compare well, both qualitatively and quantitatively, with those reported in the OGLE-III Wyrzykowski et al. (2011) τ -based analysis. They rule out sub-solar MACHOs and in particular they report an upper limit $f < 7\%$ at 95%CL for $0.4 M_{\odot}$ for the All sample, a result which is almost identical with that we reach in our analysis.

An exception to this agreement is found, on the other hand, in the mass range above $1 M_{\odot}$, in particular for the All star sample, where we estimate a relatively strong *upper* limit for the halo mass fraction, (8%, 14% and 51% for 1, 10 and $100 M_{\odot}$ respectively, at 95% CL). The driving motivation for the difference with Wyrzykowski et al. (2011) can be traced back to our larger estimate of the expected self-lensing signal, 3.49 events, to be compared with the value 2 assumed by Wyrzykowski et al. (2011) on the basis of the number of reported candidates. The larger ex-

³ The choice for the upper bound $f = 1$ is in fact relevant only for the smallest value of the MACHO mass we consider, $10^{-5} M_{\odot}$, and marginally $10^{-4} M_{\odot}$, for which in any case the OGLE-III experiment is

not very sensitive because of the sharp drop of the detection efficiency for small values of the duration.

pected self-lensing signal drives, within the framework of a confidence level estimate for a Poisson distribution with a background (Feldman & Cousins 1998), to smaller values for the upper limit on the mass halo fraction (the background signal for MACHO lensing being that of self lensing). A second reason is the likelihood analysis we carry out where, in particular, besides the number of the reported candidate events one takes into account also their *duration*. Given the observed values, about 30 days, this becomes more and more important moving towards large values for the MACHO mass, for which the expected durations are extremely large (for $100 M_{\odot}$ we evaluate a median duration of almost 500 days).

4 DISCUSSION

In this paper we have analysed the results presented in Wyrzykowski et al. (2011) for the OGLE-III microlensing campaign towards the LMC. In particular, going beyond the optical depth-based analysis of Wyrzykowski et al. (2011), but still in agreement with their conclusions, we have presented an analysis focused on the estimate of the expected number and duration of events through the evaluation of the microlensing rate for all the possible lens populations. In particular, for MACHO lensing both the MW and the LMC dark matter halo, and for self lensing, LMC disc and bar, MW disc and MW and LMC stellar haloes. As a main result we find that compact halo objects might contribute only to a negligible fraction of the dark matter haloes. In particular we evaluate a 95% CL *upper* limit for f , the halo mass fraction in form of MACHOs, in the range 10-20% for values of the mass ($10^{-2} - 0.5$) M_{\odot} , and $f = 24\%$ for $1 M_{\odot}$ (below 10% in this full range, and in particular below 5% for $(10^{-2} - 0.1) M_{\odot}$) for the Bright (All) samples of source stars. Indeed, the expected self lensing turns out to be sufficient to explain the observed signal, $N_{\text{ev}} = 2$ (both for the Bright and the All samples), with 1.37 (3.49) expected events for the Bright (All) sample, respectively. However, the number of the reported microlensing candidate events is so small compared to the number of expected MACHO lensing events, about 40 (90) for $0.1 M_{\odot}$ MACHOs for the Bright (All) sample of stars, respectively, that the limits on the halo fraction would not change much even assuming the events *are* MACHOs. A interesting outcome of the present analysis is the relatively significant upper limit on the halo mass fraction we obtain in the mass range above $1 M_{\odot}$, at least for the All sample (8%, 14% and 51% for 1, 10 and $100 M_{\odot}$, respectively). This is a stronger constraint with respect to those reported in previous microlensing analyses (Alcock et al. 2001; Tisserand et al 2007) and also in the OGLE-III analysis of Wyrzykowski et al. (2011), and fills the gap, from the microlensing side, with the upper limit from the analysis of halo wide binaries (Yoo et al. 2004). Stressing the caveat that this outcome holds for the All sample only, we also recall the event reported towards the SMC, OGLE-2005-SMC-001, for which there is evidence in favour for the lens being a heavy mass (about $10 M_{\odot}$) compact halo object (Dong et al. 2007). Finally, we have also evaluated the limits for the joint OGLE-II and OGLE-III analyses, in particular for the Bright sample of stars they remain almost unchanged.

A further relevant result of the present analysis is the role played by the MW disc population, for which we find the expected lensing signal to be almost as large as that of LMC self lensing, with a 50% contribution from the thick disc component. In particular we evaluate 0.45 and 1.14 expected events, for the Bright and the All sample respectively (against 0.63 and 1.60 for LMC self

lensing). Comparing to the two reported candidate events, both the LMC and the MW disc stars might explain the observed signal. In fact, for the All sample, the observed rate is smaller, though still fully compatible, than the overall expected self lensing signal (3.49 events including the stellar halo components).

These results, although they look quite conclusive on the MACHOs contribution, at least for the mass range $(0.1 - 1) M_{\odot}$, still leave a few open issues. First, the statistics of the observed events is still too small to carry out a meaningfully analysis on their observed characteristics, as duration and spatial distribution, so to draw stringent conclusions on the exact nature of the lenses. The observed durations, around 30 days, are shorter than the averaged expected durations for LMC self lensing, which could still however, based on their expected number, explain both the observed events. At least one event, however, both for its position, in the outer LMC region, and duration, looks more easily explained by the Galactic disc population. Durations and positions are on the other hand also compatible with MACHO lensing, especially in the mass range $(0.1 - 1) M_{\odot}$; furthermore, the spatial distribution might be suggestive of an asymmetry compatible with that expected by the LMC dark matter halo (Calchi Novati et al. 2006). Again, however, the overall statistics of events is too small to further address this issue.

The number of reported candidates is the final outcome of the selection pipeline. It is beyond the purpose of this paper to address this issue, still we stress the potential difficulty within the evaluation of the detection efficiency to correctly take into account the risk of excluding bona fide microlensing candidates (as with the χ^2 cut which severely reduces the number of viable candidates in the OGLE analyses). To better address this issue, whose importance is strongly enhanced by the very small number of candidate events reported, we believe that a full achromatic-based 2-bands analysis (even though complicated by the blending effect) would greatly help to more easily distinguish microlensing from intrinsic variables, and hopefully to lead more easily to a larger set of reliable candidate events. After the OGLE-II and OGLE-III campaign, for which essentially the pipeline was carried out with *I*-band data only, we hope the ongoing OGLE-IV may therefore adopt this strategy.

For both its OGLE-II and OGLE-III LMC campaigns OGLE choosed to present its results for both a, smaller, “Bright” and a “All” sample of source stars. The underlying reason for this choice is linked to the central issue of *blending*. OGLE-II reported 0 and 2 events out of the Bright and All sample selection pipelines, respectively, whereas OGLE-III reported 2 events for both samples. The expected self-lensing rate is of 0.64 (1.49) for OGLE-II and 1.37 (3.49) for OGLE-III, for the Bright (All) sample, respectively. Once again, the overall small statistics is too small, however it is clear that this two-sample strategy might be taken as an opportunity for a strong internal self-consistency check of the full analysis (selection pipeline, efficiency and evaluation of the number of sources). Here again, the ongoing OGLE-IV campaign has the chance of going beyond these previous analyses. The obvious strategy for enhancing the microlensing rate is to allow for fainter sources, in particular within the All sample, even at the risk of complicating the blending analysis.

Finally, we have discussed the strategy of the OGLE-II and OGLE-III campaigns as compared to the previous ones carried out by the MACHO and the EROS collaborations. Given the caveats discussed above, it is clear that the results obtained by OGLE, in agreement with those of EROS (Tisserand et al 2007) do not leave much place to a significant compact halo objects population. It remains increasingly difficult therefore to explain, within this framework, the results of MACHO (Alcock et al. 2000; Bennett 2005).

A possible way out is, once more, that of a significant increase in the expected statistics for self-lensing events, so to allow one to use them as a strong test case to be compared with the expected MACHO lensing signal. In this respect the ongoing OGLE-IV campaign (Udalski 2011), with its still increased overall field of view, the MOA campaign (Sumi 2011), as well as SuperMACHO (Rest et al. 2005), might hopefully help to definitively address at least the issue of the contribution of faint compact objects and fill the gap between the MACHO and the EROS strategies and results.

ACKNOWLEDGMENTS

We are grateful to the referee for interesting suggestions and remarks that helped us to improve the manuscript. We warmly thank Ł. Wyrzykowski for carefully reading the manuscript, useful discussions and comments as well as for making available to us some unpublished data of its analysis. We acknowledge support by MIUR through PRIN 2008 prot. 2008NR3EBK.

REFERENCES

- Alcock C. et al., 1993, *Nature*, 365, 621
 Alcock C. et al., 1999, *ApJ*, 518, 44
 Alcock C. et al., 2000, *ApJ*, 542, 281
 Alcock C. et al., 2001a, *ApJSS*, 136, 439
 Alcock C. et al., 2001b, *ApJ*, 550, L169
 Alcock C. et al., 2001c, *Nature*, 414, 617
 Alves D. R., 2004, *ApJ*, 601, L151
 Aubourg E. et al., 1993, *Nature*, 365, 623
 Bekki K., 2011, *ApJ*, 730, L2
 Bennett D. P., 2005, *ApJ*, 633, 906
 Bozza V., Calchi Novati S., Mancini L., Scarpetta G. (Eds.), 2011, XV International Conference on Gravitational Microlensing: Conference Book, arXiv:1102.0452
 Calchi Novati S., 2010, *General Relativity and Gravitation*, 42, 2101 (Invited review)
 Calchi Novati S. et al., 2005, *A&A*, 443, 911
 Calchi Novati S., De Luca F., Jetzer P., Scarpetta G., 2006, *A&A*, 459, 407
 Calchi Novati S., de Luca F., Jetzer P., Mancini L., Scarpetta G., 2008, *A&A*, 480, 723
 Calchi Novati S., Mancini L., Scarpetta G., Wyrzykowski Ł., 2009, *MNRAS*, 400, 1625
 de Jong J. T. A., Yanny B., Rix H.-W., Dolphin A. E., Martin N. F., Beers T. C., 2010, *ApJ*, 714, 663
 Dehnen W., Binney J., 1998, *MNRAS*, 294, 429
 Dong S. et al., 2007, *ApJ*, 664, 862
 Drake A. J., Cook K. H., Keller S. C., 2004, *ApJ*, 607, L29
 Feldman G. J., Cousins R. D., 1998, *Phys. Rev. D*, 57, 3873
 Flynn C., Holmberg J., Portinari L., Fuchs B., Jahreiß H., 2006, *MNRAS*, 372, 1149
 Gould A., 1994, *ApJ*, 421, L71
 Gould A., 1996, *ApJ*, 470, 201
 Gould A., 2004, *ApJ*, 606, 319
 Gould A., Miralda-Escude J., Bahcall J. N., 1994, *ApJ*, 423, L105
 Gould A., Bennett D. P., Alves D. R., 2004, *ApJ*, 614, 404
 Gyuk G., Dalal N., Griest K., 2000, *ApJ*, 535, 90
 Hamadache C. et al., 2006, *A&A*, 454, 185
 Jetzer P., Mancini L., Scarpetta G., 2002, *A&A*, 393, 129
 Jurić M. et al., 2008, *ApJ*, 673, 864
 Kroupa P., 2007, The initial mass function of simple and composite stellar populations, astro-ph/0703124
 Mancini L., 2009, *A&A*, 496, 465
 Mancini L., Calchi Novati S., Jetzer P., Scarpetta G., 2004, *A&A*, 427, 61
 Mao S., 2008, Introduction to Microlensing, in Proceedings of the Manchester Microlensing Conference: The 12th International Conference and ANGLES Microlensing Workshop, Eds. E. Kerins, S. Mao, N. Rattenbury and Ł. Wyrzykowski, PoS(GMC8)002, arXiv:0811.0441,
 Moniez M., 2010, *General Relativity and Gravitation*, 42, 2047 (Invited review)
 Paczyński B., 1986, *ApJ*, 304, 1
 Pejcha O., Stanek K. Z., 2009, *ApJ*, 704, 1730
 Popowski P. et al., 2005, *ApJ*, 631, 879
 Rest A. et al., 2005, *ApJ*, 634, 1103
 Rhie S. H., Becker A. C., Bennett D. P., Fragile P. C., Johnson B. R., King L. J., Peterson B. A., Quinn J., 1999, *ApJ*, 522, 1037
 Sahu K. C., 1994, *Nature*, 370, 275
 Sahu K. C., Sahu M. S., 1998, *ApJ*, 508, L147
 Smith M. C., Woźniak P., Mao S., Sumi T., 2007, *MNRAS*, 380, 805
 Subramanian S., Subramaniam A., 2010, *A&A*, 520, A24+
 Sumi T., 2011, in XV International Conference on Gravitational Microlensing: Conference Book, V. Bozza, S. Calchi Novati, L. Mancini and G. Scarpetta (Eds.), arXiv:1102.0452, p. 20
 Sumi T. et al., 2003, *ApJ*, 591, 204
 Sumi T. et al., 2006, *ApJ*, 636, 240
 Tisserand P. et al., 2007, *A&A*, 469, 387
 Udalski A., 2011, in XV International Conference on Gravitational Microlensing: Conference Book, V. Bozza, S. Calchi Novati, L. Mancini and G. Scarpetta (Eds.), arXiv:1102.0452, p. 19
 Udalski A. et al., 1993, *Acta Astronomica*, 43, 289
 van der Marel R. P., Alves D. R., Hardy E., Suntzeff N. B., 2002, *AJ*, 124, 2639
 Wyrzykowski Ł. et al., 2009, *MNRAS*, 397, 1228
 Wyrzykowski Ł. et al., 2010, *MNRAS*, 407, 189
 Wyrzykowski Ł. et al., 2011, *MNRAS*, 413, 493
 Yoo J., Chanamé J., Gould A., 2004, *ApJ*, 601, 311